

# Octupole correlations in low-lying states of $^{150}\text{Nd}$ and $^{150}\text{Sm}$ and their impact on neutrinoless double-beta decay

J. M. Yao\* and J. Engel

*Department of Physics and Astronomy, University of North Carolina, Chapel Hill, NC 27516-3255, USA*

We present a generator-coordinate calculation, based on a relativistic energy-density functional, of the low-lying spectra in the isotopes  $^{150}\text{Nd}$  and  $^{150}\text{Sm}$  and of the nuclear matrix element that governs the neutrinoless double-beta decay of the first isotope to the second. We carefully examine the impact of octupole correlations on both nuclear structure and the double-beta decay matrix element. Octupole correlations turn out to reduce quadrupole collectivity in both nuclei. Shape fluctuations, however, dilute the effects of octupole deformation on the double-beta decay matrix element, so that the overall octupole-induced quenching is only about 7%.

PACS numbers: 21.60.Jz, 24.10.Jv, 23.40.Bw, 23.40.Hc

## I. INTRODUCTION

The nucleus  $^{150}\text{Nd}$  has been the active isotope in double-beta ( $\beta\beta$ ) decay experiments [1], and may be again in the future [2]. It has  $N = 90$  neutrons and is part of a set of isotones in which nuclear structure changes rapidly as neutrons are added or removed. Ref. [3] showed that the low-lying states of  $^{150}\text{Nd}$  and other  $N = 90$  isotones are close to the predictions of the X(5) model, which describes the critical point of a first order phase transition from spherical harmonic vibrator to axially-deformed rotor. A significant amount of work on nuclear phase transitions in the  $N \simeq 90$  isotones followed this discovery [4–11]. We concern ourselves here, however, with a different aspect of structure in  $^{150}\text{Nd}$ : octupole correlations, suggested by the observation of low-lying negative-parity states and fast  $E3$  transitions [12–14]. Refs. [15–21] applied a wide variety of models with octupole shape degrees of freedom to nuclei with  $N \simeq 90$ . The models indicated that the proton  $1h_{11/2}$ – $2d_{5/2}$  and neutron  $1i_{13/2}$ – $2f_{7/2}$  orbitals near the Fermi levels are responsible for the strong octupole correlations. And very recently the authors of Refs. [22, 23] used the *sdf* interacting Boson model (IBM), with Hamiltonian parameters determined from self-consistent mean-field calculations, to successfully describe the low-lying states of  $N \simeq 90$  nuclei. These studies imply that the low-lying states of  $^{150}\text{Nd}$  are dominated by the quadrupole-octupole collective excitations and that the EDF approaches provide good basis states for them.

The *sdf* IBM calculation [22, 23] can be regarded — very roughly speaking — as something like an EDF-based shell-model calculation with the model space truncated to states constructed from nucleon pairs with angular momentum  $J = 0, 2$ , and  $3$ . It obviously contains correlations beyond those of mean-field theory. In this paper, we carry out a symmetry-projected beyond-

mean-field calculation, using the Generator Coordinate Method (GCM) to study the low-lying states of  $^{150}\text{Nd}$  and  $^{150}\text{Sm}$  and to quantify the effects of octupole correlations on the matrix element that governs neutrinoless double-beta ( $0\nu\beta\beta$ ) decay from the ground state of the first to that of the second. Our starting point is a self-consistent relativistic mean-field (RMF) calculation [24–27] with constraints on both quadrupole and octupole mass moments, part of a framework that has already been used to study static octupole deformation in nuclear ground states [19, 28–31]. The GCM approach we take here (also known as multi-reference covariant density-functional theory) allows us to go beyond mean-field theory, however, by including dynamical correlations associated with symmetry restoration and shape fluctuations [32–38]. Octupole shape fluctuations [39, 40] have not yet been studied extensively. Previous work on the  $\beta\beta$  decay of  $^{150}\text{Nd}$  has shown that the matrix elements are sensitive to quadrupole deformation [41–48]. It is the effect of octupole correlations that we address here.

This paper is organized as follows: Section II briefly presents the RMF theory that we use to generate reference states, the GCM and several projection techniques that we apply to nuclear collective quadrupole and octupole excitations, and the formulae for computing the matrix elements of the operator responsible for  $0\nu\beta\beta$  decay. Section III presents our results for the structure of low-lying states in  $^{150}\text{Nd}$  and  $^{150}\text{Sm}$ , and for the  $0\nu\beta\beta$  matrix elements, which we compare with those of previous studies that neglect octupole degrees of freedom. Section IV summarizes our findings.

## II. THE MODEL

### A. Generating mean-field reference states in collective coordinate space

The first step in the GCM procedure is to generate a set of collective reference (or basis) states  $|q\rangle$ . We do so by carrying out constrained mean-field calculations based with a relativistic point-coupling energy-density

---

\*On leave from School of Physical Science and Technology, Southwest University, 400715 Chongqing, China

functional (EDF) [49–51]:

$$E_{\text{RMF}} = \int d\mathbf{r} \mathcal{E}_{\text{RMF}}[\rho, j], \quad (1)$$

where  $\mathcal{E}_{\text{RMF}}$  is defined as

$$\begin{aligned} \mathcal{E}_{\text{RMF}}[\rho, j] = & \sum_{k,\tau} v_{k,\tau}^2 \bar{\psi}_{k,\tau}(\mathbf{r}) (-i\boldsymbol{\gamma}\nabla + m) \psi_{k,\tau}(\mathbf{r}) \\ & + \frac{\alpha_0}{2} \rho^2 + \frac{\beta_0}{3} \rho^3 + \frac{\gamma_0}{4} \rho^4 + \frac{\delta_0}{2} \rho \Delta \rho \\ & + \frac{\alpha_1}{2} j_\mu j^\mu + \frac{\gamma_1}{4} (j_\mu j^\mu)^2 + \frac{\alpha_{11}}{2} \tilde{j}^\mu \tilde{j}_\mu \\ & + \frac{\delta_1}{2} j_\mu \Delta j^\mu + \frac{\delta_{11}}{2} \tilde{j}^\mu \Delta \tilde{j}_\mu \\ & + \frac{\alpha_{10}}{2} \tilde{\rho}^2 + \frac{\delta_{10}}{2} \tilde{\rho} \Delta \tilde{\rho} + \frac{1}{4} e (j_\mu - \tilde{j}_\mu) A^\mu. \end{aligned} \quad (2)$$

Here  $\tau = 1$  (neutron) or  $-1$  (proton),  $\psi_{k,\tau}$  is the Dirac wave function for the  $k^{\text{th}}$  nucleon with isospin  $\tau$ , and  $A^\mu$  is the electromagnetic field. The functional contains eleven constants  $\alpha$ ,  $\beta$ ,  $\gamma$  and  $\delta$ . The local isoscalar and isovector densities  $\rho$  and  $\tilde{\rho}$ , and the corresponding isoscalar and isovector currents  $j_\mu$  and  $\tilde{j}_\mu$  are

$$\rho(\mathbf{r}) = \sum_{k,\tau} v_{k,\tau}^2 \bar{\psi}_{k,\tau}(\mathbf{r}) \psi_{k,\tau}(\mathbf{r}), \quad (3a)$$

$$\tilde{\rho}(\mathbf{r}) = \sum_{k,\tau} \tau v_{k,\tau}^2 \bar{\psi}_{k,\tau}(\mathbf{r}) \psi_{k,\tau'}(\mathbf{r}), \quad (3b)$$

$$j^\mu(\mathbf{r}) = \sum_{k,\tau} v_{k,\tau}^2 \bar{\psi}_{k,\tau}(\mathbf{r}) \boldsymbol{\gamma}^\mu \psi_{k,\tau}(\mathbf{r}), \quad (3c)$$

$$\tilde{j}^\mu(\mathbf{r}) = \sum_{k,\tau} \tau v_{k,\tau}^2 \bar{\psi}_{k,\tau}(\mathbf{r}) \boldsymbol{\gamma}^\mu \psi_{k,\tau}(\mathbf{r}). \quad (3d)$$

These quantities are calculated in the *no-sea* approximation, i.e. with the summation in Eqs. (3a) – (3d) running over all states with  $v_{k,\tau}^2 > 0$ , where the  $v_{k,\tau}^2$  is the occupation probability for the  $k^{\text{th}}$  nucleon of type  $\tau$  in the BCS wave function

$$|q\rangle = \prod_{k>0,\tau} (u_{k,\tau} + v_{k,\tau} c_{k,\tau}^\dagger c_{k,\tau}^\dagger) |0\rangle. \quad (4)$$

The numbers  $u_{k,\tau}$  and  $v_{k,\tau}$  obey  $u_{k,\tau}^2 + v_{k,\tau}^2 = 1$ . The operator  $c_{k,\tau}^\dagger$  creates a nucleon of type  $\tau$  in the single-nucleon state  $k$ . The corresponding spinor  $\psi_{k,\tau}$  is determined by the variational principle

$$\delta \langle q | \hat{H} - \sum_\tau \lambda_\tau \hat{N}_\tau - \sum_{\lambda=1,2,3} C_\lambda (\hat{Q}_{\lambda 0} - q_\lambda)^2 | q \rangle = 0, \quad (5)$$

with the Lagrange multipliers  $\lambda_\tau$  fixed by the constraints  $\langle q | \hat{N}_1 | q \rangle = N$  and  $\langle q | \hat{N}_{-1} | q \rangle = Z$ . The deformation parameters  $\beta_\lambda$  ( $\lambda = 2, 3$ ) are related to the mass multipole moments by

$$\beta_\lambda \equiv \frac{4\pi}{3AR^\lambda} q_\lambda, \quad R = 1.2A^{1/3}, \quad (6)$$

with  $A$  representing the mass number of the nucleus under consideration.

We iteratively solve the Dirac equation derived from (5) by expanding the Dirac spinors  $\psi_{k,\tau}$  in a basis of single-particle oscillator states within 12 shells [52]. As Eq. (4) indicates, we treat pairing correlations in the BCS approximation, with a density-independent zero-range pairing interaction [53]. We always employ the relativistic energy density functional PC-PK1 [51]. Previous symmetry-projected GCM studies [7, 46] have shown that the low-lying states produced by the PC-PK1 and the PC-F1 [50] are close to each other in energy, suggesting that reasonable changes in the particle-hole structure of the energy-density functional will not produce major changes in low-lying structure. The pairing functional, however, has been shown to have a significant effect in  $^{150}\text{Nd}$ , on both in its collective structure [54] and its matrix element for neutrinoless double beta decay [46]. Here, as in Ref. [46] we choose to fit the pairing strengths to the average pairing gaps produced by a separable finite-range pairing force at the mean-field energy minimum [55]. The procedure leads to pairing gaps that are similar to those obtained both from the Gogny functional and experiment.

## B. Symmetry restoration and configuration mixing

We construct physical state vectors  $|J_\alpha^\pi\rangle$  by superposing projected mean-field reference states:

$$|J_\alpha^\pi\rangle = \sum_q f_q^{J\pi\alpha} |JM\pi NZ; q\rangle, \quad (7)$$

where  $|JM\pi NZ; q\rangle \equiv \hat{P}_{M0}^J \hat{P}^N \hat{P}^Z \hat{P}^\pi |q\rangle$ , with the “0” in the first projector corresponding to the intrinsic quantum number  $K$  (which will be zero for all our states) and the collective coordinate  $q$  standing for the intrinsic deformation parameters  $(\beta_2, \beta_3)$  of the reference states. The  $\hat{P}$ ’s are projection operators onto states with well-defined angular momentum  $J$  and its  $z$ -component  $M$ , parity ( $\pi = \pm$ ), and neutron and proton number  $(N, Z)$  [56]. [ $N$ ,  $Z$ , and  $K$  are implied on the left-hand side of Eq. (7)]. The weight functions  $f_q^{J\pi\alpha}$ , where  $\alpha$  is a simple enumeration index, are solutions to the Hill-Wheeler-Griffin equation [57, 58]

$$\sum_{q'} [\mathcal{H}_{q,q'}^{J\pi} - E_\alpha^{J\pi} \mathcal{N}_{q,q'}^{J\pi}] f_{q'}^{J\pi\alpha} = 0, \quad (8)$$

where the Hamiltonian kernel  $\mathcal{H}_{q,q'}^{J\pi}$  and the norm kernel  $\mathcal{N}_{q,q'}^{J\pi}$  are given by

$$\left\{ \begin{array}{c} \mathcal{H} \\ \mathcal{N} \end{array} \right\}_{q,q'}^{J\pi} = \langle q | \left\{ \begin{array}{c} \hat{H} \\ 1 \end{array} \right\} \hat{P}_{00}^J \hat{P}^N \hat{P}^Z \hat{P}^\pi | q' \rangle, \quad (9)$$

To solve Eq. (8), we first diagonalize the norm kernel  $\mathcal{N}$  and then use the non-zero eigenvalues and corresponding

eigenvectors to construct the “natural basis” [36, 56, 59]. We re-diagonalize the Hamiltonian in that basis to obtain the states  $|J_\alpha^\pi\rangle$  and the energies  $E_\alpha^{J^\pi}$ .

Because we begin with an energy functional rather than a Hamiltonian, we need a prescription for the off-diagonal matrix elements of  $\mathcal{H}$ . Following standard practice, we simply replace the diagonal density in the functional by the transition density. Though the prescription brings with it spurious divergences and “steps” [60, 61], it does not produce an unresolvable ambiguity when used together with the relativistic EDF in Eq. (1), which contains only integer powers of the density. We exclude exchange terms but avoid numerical instabilities in particle-number projection at the gauge angle  $\phi = \pi/2$  by setting  $L$  to 9 in Fomenko’s expansion [62]. Refs. [32, 36, 59, 63, 64] contain detailed discussions of beyond-mean-field calculations with energy-density functionals.

### C. Nuclear matrix element for $0\nu\beta\beta$ decay

The  $0\nu\beta\beta$  decay nuclear matrix element is

$$M^{0\nu} = \frac{4\pi R}{g_A^2(0)} \int \int d^3x_1 d^3x_2 \int \frac{d^3q}{(2\pi)^3} \frac{e^{i\mathbf{q}\cdot(\mathbf{x}_1-\mathbf{x}_2)}}{q} \times \sum_m \frac{\langle 0_F^+ | \mathcal{J}_\mu^\dagger(\mathbf{x}_1) | m \rangle \langle m | \mathcal{J}^{\mu\dagger}(\mathbf{x}_2) | 0_I^+ \rangle}{q + E_m - (E_I + E_F)/2}, \quad (10)$$

where  $\mathcal{J}_\mu^\dagger$  is the charge-changing nuclear current operator [65] and  $q$  is the momentum transferred from leptons to nucleons. The nuclear radius  $R = 1.2A^{1/3}$  makes the matrix element dimensionless. In the closure approximation and with the GCM state vectors from Eq. (7) as ground states  $|0_{I/F}^+\rangle$  of the initial and final nuclei, we obtain

$$M^{0\nu} = \sum_{q_I, q_F} f_{q_I}^{0_I^+} f_{q_F}^{0_F^+} \langle q_F | \hat{O}^{0\nu} \hat{P}^{J=0} \hat{P}^N \hat{P}^Z \hat{P}^{\pi=+} | q_I \rangle, \quad (11)$$

with the transition operator given by

$$\hat{O}^{0\nu} = \frac{4\pi R}{g_A^2(0)} \int \frac{d^3q}{(2\pi)^3} \int \int d^3x_1 d^3x_2 \frac{e^{i\mathbf{q}\cdot(\mathbf{x}_1-\mathbf{x}_2)}}{q(q+E_d)} \times [\mathcal{J}_\mu^\dagger(\mathbf{x}_1) \mathcal{J}^{\mu\dagger}(\mathbf{x}_2)], \quad (12)$$

and  $E_d$  set to  $1.12A^{1/2} \simeq 13.72$  Mev [66].

The operator  $[\mathcal{J}_\mu^\dagger(\mathbf{x}_1) \mathcal{J}^{\mu\dagger}(\mathbf{x}_2)]$ , when Fourier transformed, contains the terms [46],

$$\begin{aligned} VV : & \quad g_V^2(\mathbf{q}^2) (\bar{\psi}\gamma_\mu\tau_-\psi)^{(1)} (\bar{\psi}\gamma^\mu\tau_-\psi)^{(2)} \\ AA : & \quad g_A^2(\mathbf{q}^2) (\bar{\psi}\gamma_\mu\gamma_5\tau_-\psi)^{(1)} (\bar{\psi}\gamma^\mu\gamma_5\tau_-\psi)^{(2)} \\ AP : & \quad 2g_A(\mathbf{q}^2)g_P(\mathbf{q}^2) (\bar{\psi}\gamma\gamma_5\tau_-\psi)^{(1)} (\bar{\psi}\mathbf{q}\gamma_5\tau_-\psi)^{(2)} \\ PP : & \quad g_P^2(\mathbf{q}^2) (\bar{\psi}\mathbf{q}\gamma_5\tau_-\psi)^{(1)} (\bar{\psi}\mathbf{q}\gamma_5\tau_-\psi)^{(2)} \\ MM : & \quad g_M^2(\mathbf{q}^2) \left( \bar{\psi} \frac{\sigma_{\mu i}}{2m_N} q^i \tau_-\psi \right)^{(1)} \left( \bar{\psi} \frac{\sigma^{\mu j}}{2m_N} q_j \tau_-\psi \right)^{(2)}, \end{aligned} \quad (13)$$

where  $\tau_-$  is the isospin lowering operator that changes neutrons into protons,  $\sigma_{\mu\nu} = \frac{1}{2}[\gamma_\mu, \gamma_\nu]$ , and  $V, A, P, M$  denote the vector, axial vector, pseudoscalar, and magnetic pieces of the one-nucleon current. Following Ref. [67], we take the form factors  $g_V(\mathbf{q}^2)$ ,  $g_A(\mathbf{q}^2)$ ,  $g_M(\mathbf{q}^2)$ , and  $g_P(\mathbf{q}^2)$  to be

$$g_V(\mathbf{q}^2) = \frac{g_V(0)}{(1 + \mathbf{q}^2/\Lambda_V^2)^2}, \quad (14a)$$

$$g_A(\mathbf{q}^2) = \frac{g_A(0)}{(1 + \mathbf{q}^2/\Lambda_A^2)^2}, \quad (14b)$$

$$g_P(\mathbf{q}^2) = g_A(\mathbf{q}^2) \frac{2m_N}{\mathbf{q}^2 + m_\pi^2} \left(1 - \frac{m_\pi^2}{\Lambda_A^2}\right), \quad (14c)$$

$$g_M(\mathbf{q}^2) = (\mu_p - \mu_n)g_V(\mathbf{q}^2), \quad (14d)$$

with  $g_V(0) = 1.0$ ,  $g_A(0) = 1.254$ ,  $\mu_p - \mu_n = 3.70$ ,  $\Lambda_V^2 = 0.710$  (GeV)<sup>2</sup>,  $\Lambda_A = 1.09$  GeV,  $m_N = 0.93827$  GeV and  $m_\pi = 0.13957$  GeV. For the sake of simplicity, we neglect short-range correlations.

We include, alongside the generator coordinates from Ref. [46], the octupole deformation parameter  $\beta_3$ . The parity breaking (and subsequent projection) and the larger number of reference states caused by the inclusion of octupole deformation increase computing time but otherwise cause no problems in our calculation. We initially include 50 reference states with  $\beta_3 > 0$ . From this set, 29 natural states turn out to be sufficient to include essentially all the contributions of the original 50 states to both structure properties and  $0\nu\beta\beta$  decay matrix elements.

## III. RESULTS AND DISCUSSION

Figure 1 shows the mean-field and quantum-number-projected energy surfaces, as well as the collective wave functions  $|g_\alpha^J(q)|^2$ , for the ground states of <sup>150</sup>Nd and <sup>150</sup>Sm. The collective wave functions, defined as  $g_\alpha^{J^\pi}(q) \equiv \sum_{q'} [\mathcal{N}_{q,q'}^{J^\pi}]^{1/2} f_{q'}^{J^\pi\alpha}$ , provide information about the importance of deformation in the state  $|J_\alpha^\pi\rangle$ . The mean-field energy surfaces in both nuclei around the quadrupole-deformed minima with  $\beta_2$  around 0.2 are almost flat in the octupole direction. This kind of surface often signifies a critical point symmetry [5, 7, 11]. Our surface, however, is flat only before projection of the states that determine it onto the subspace with  $J^\pi = 0^+$  and well-defined  $N$  and  $Z$ ; after projection it shows pronounced minima around  $\beta_3 \sim 0.1$ . This is a genuine effect, arising from the restoration of the symmetries spontaneously broken at the mean-field level. In addition, valleys connect the prolate and oblate minima through octupole shapes in both nuclei. As a result, the collective wave functions are shifted towards smaller quadrupole deformation via the octupole coordinate; quadrupole collectivity is thus reduced and octupole shape fluctuations are large.

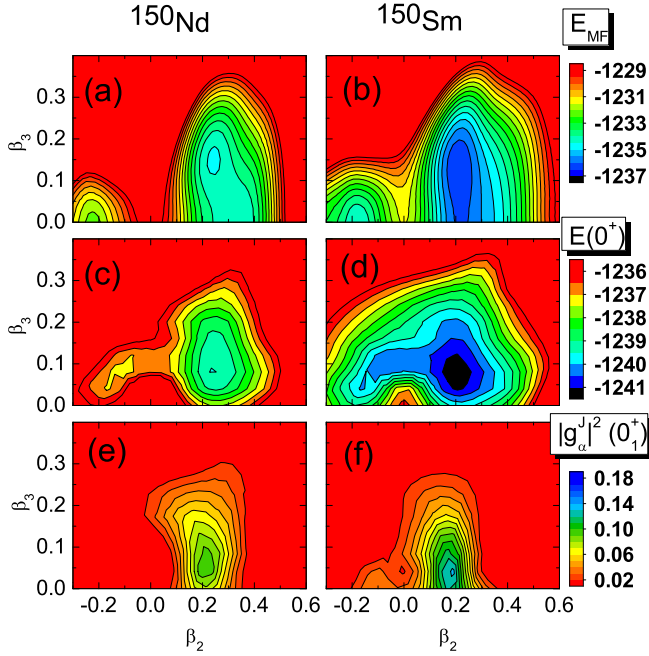


FIG. 1: (Color online) Mean-field energy surfaces for  $^{150}\text{Nd}$  (a) and  $^{150}\text{Sm}$  (b), projected energy surfaces for  $^{150}\text{Nd}$  (c) and  $^{150}\text{Sm}$  (d), and the square of the collective ground-state wave function for  $^{150}\text{Nd}$  (e) and  $^{150}\text{Sm}$  (f), all in the  $\beta_2$ - $\beta_3$  plane.

Figure 2 shows the low-lying energy spectra in  $^{150}\text{Nd}$  and  $^{150}\text{Sm}$ . The octupole degree of freedom reduces the  $E2$  transition strengths between positive-parity states significantly in both nuclei. It worsens the agreement in  $^{150}\text{Nd}$  but improves it in  $^{150}\text{Sm}$ . Our GCM describes the negative-parity band built on the  $1^-$  state rather well, despite overestimating the transition strength  $B(E3 : 0_1^+ \rightarrow 3_1^-)$  in  $^{150}\text{Nd}$  and underestimating it in  $^{150}\text{Sm}$ .

Figure 3 compares the GCM excitation energies with those calculations that use a single symmetry-projected BCS state, either the one that corresponds to the  $J = 0$  energy minimum or the one with deformation parameters determined by the experimental  $B(E2 : 0_1^+ \rightarrow 2_1^+)$  and  $B(E3 : 0_1^+ \rightarrow 3_1^-)$  values [68]. The GCM results that include the configuration-mixing effect are in much better agreement with the data than those based on a single BCS state. As spin increases, however, the GCM increasingly over-predicts the data, indicating that some important correlations are missing. Time-reversal-symmetry-breaking reference states, produced in a cranking calculation, would likely lower the energies of high-spin states [69].

Figure 4 displays the normalized  $0\nu\beta\beta$  matrix element between reference states, which we denote by  $\tilde{M}^{0\nu}(q_I, q_F)$ :

$$\tilde{M}^{0\nu}(q_I, q_F) \equiv \frac{\langle q_F | \hat{C}^{0\nu} \hat{P}^{J=0} \hat{P}^{N_I} \hat{P}^{Z_I} P^{\pi=+} | q_I \rangle}{\sqrt{\mathcal{N}_{q_I}^{0+} \mathcal{N}_{q_F}^{0+}}}, \quad (15)$$

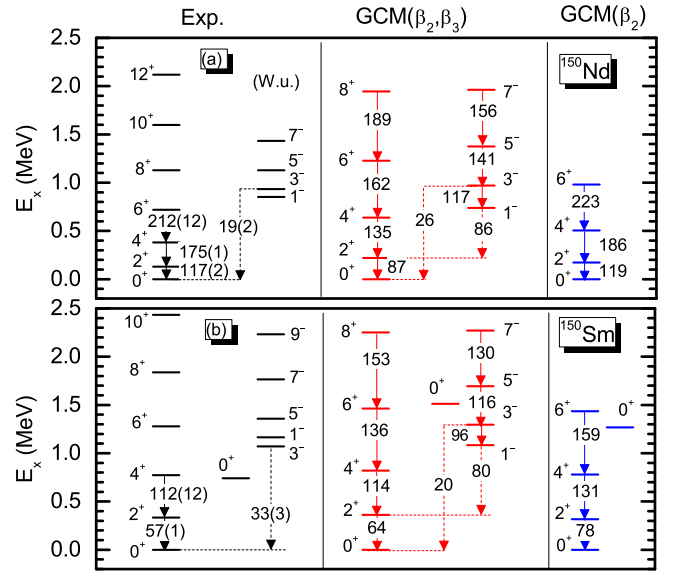


FIG. 2: (Color online) Low-energy spectra of  $^{150}\text{Nd}$  and  $^{150}\text{Sm}$ . The numbers on arrows are  $E2$  (solid line) and  $E3$  (dashed line) transition strengths, in Weisskopf units. Data are from Ref. [68].

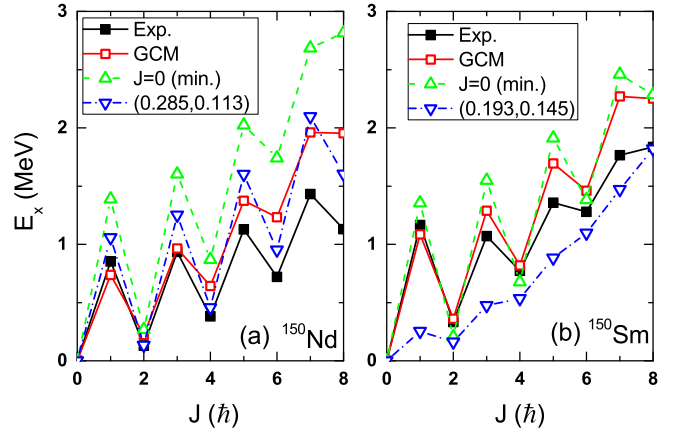


FIG. 3: (Color online) Excitation energies of parity doublet states in  $^{150}\text{Nd}$  (a) and  $^{150}\text{Sm}$  (b). The available data (■) are compared with the GCM results (□) and the results produced by the single-configuration of  $J = 0$  energy minimum (△) and by the configuration with deformation parameters determined by measured transition strengths  $B(E2 : 0_1^+ \rightarrow 2_1^+)$  and  $B(E3 : 0_1^+ \rightarrow 3_1^-)$  (▽) [68].

with the norms  $\mathcal{N}$  for each nucleus defined in Eq. (9). The function  $\tilde{M}^{0\nu}(q_I, q_F)$  represents the contribution of particular initial and final configurations to the full matrix element. Panel (a) of Fig. 4 plots the function in the  $\beta_3^I, \beta_3^F$  plane, with  $\beta_2^I$  and  $\beta_2^F$  fixed at 0.2, the value that minimizes the energy in both nuclei. The figure shows that unequal octupole deformation in the two nuclei causes a rapid drop in the  $0\nu\beta\beta$  matrix element. Panel (b) of Fig. 4 extracts the behavior of  $\tilde{M}^{0\nu}$  from the diagonal of panel (a), where the octupole deforma-

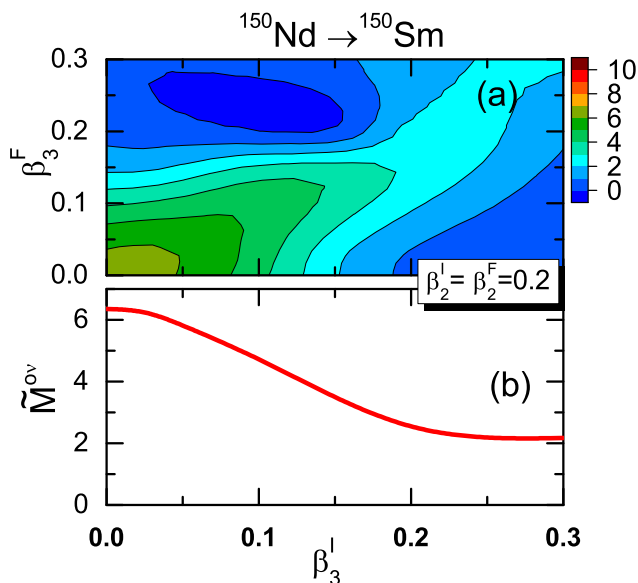


FIG. 4: (Color online) Normalized nuclear matrix elements  $\tilde{M}^{0\nu}(q_I, q_F)$  for the neutrinoless double-beta decay of  $^{150}\text{Nd}$ , where  $\{q\} \equiv \{\beta_2, \beta_3\}$ . Panel (a) plots  $\tilde{M}^{0\nu}$  versus the initial and final octupole deformation parameters, with the quadrupole deformation parameters  $\beta_2^I$  and  $\beta_2^F$  fixed at 0.2. Panel (b) plots the same quantity with the restriction  $\beta_3^I = \beta_3^F$ .

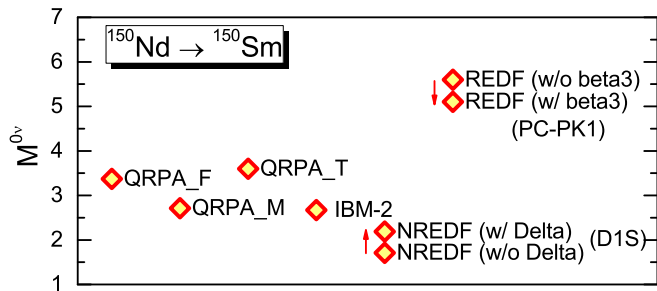


FIG. 5: (Color online) The final matrix element  $M^{0\nu}$  from the GCM calculation with and without [46] octupole shape fluctuations (REDF) and those of the QRPA (“QRPA\_F” [70], “QRPA\_M” [45], “QRPA\_T” [47]), the IBM-2 [71], and the non-relativistic GCM, based on the Gogny D1S interaction, with [72] and without [44] pairing fluctuations.

tion is the same size in both nuclei. Increasing deformation causes even this diagonal contribution to drop, from 6.4 to 2.2 as  $\beta_3$  increases to 0.3. At the configurations that minimize the projected energies, with both values of  $\beta_2$  about 0.2 and both values of  $\beta_3$  about 0.1,  $\tilde{M}^{0\nu}$  is 4.76. At the configuration that best fits the experimental  $B(E2 : 0_1^+ \rightarrow 2_1^+)$  and  $B(E3 : 0_1^+ \rightarrow 3_1^-)$  values, corresponding to deformation parameters  $\beta_2^I = 0.285$ ,  $\beta_3^I = 0.113$ ,  $\beta_2^F = 0.193$ ,  $\beta_3^F = 0.145$ ,  $\tilde{M}^{0\nu}$  is only 1.38.

As already discussed in Refs. [46, 48],  $\tilde{M}^{0\nu}$  near spherical shapes is much larger than predicted by the Gogny D1S interaction [44]. The difference arises at least in part

from a difference in average pairing gaps, which for the neutrons in  $^{150}\text{Nd}$  and  $^{150}\text{Sm}$  are about 30% larger here than in Ref. [44] (even though the gaps are similar at the mean-field minima).

When all configurations are appropriately combined, we obtain a final value for the matrix element  $M^{0\nu}(0_1^+ \rightarrow 0_1^+)$  of 5.2, which is just 7% smaller than the result 5.6 obtained without octupole deformation [46]. (The contributions from the  $VV$ ,  $AA$ ,  $AP$ ,  $PP$ , and  $MM$  terms are 1.03, 4.87,  $-1.65$ , 0.70, and 0.21, respectively). The small reduction, significantly less than what would result from the use of the single configuration in each nucleus that minimizes the energy (4.76) shows that shape fluctuations wash out the effects of octupole deformation. For the  $0\nu\beta\beta$  decay to the excited  $0_2^+$  state in  $^{150}\text{Sm}$ , we find  $M^{0\nu}(0_1^+ \rightarrow 0_2^+) = 0.72$ .

Figure 5 compares the ground-state to ground-state matrix elements  $M^{0\nu}(0_1^+ \rightarrow 0_1^+)$  from several models. Our relativistic EDF-based GCM result is still about twice those of the deformed quasiparticle random phase approximation (QRPA) and the interacting boson model (IBM), and about three times that of the non-relativistic Gogny-based GCM. A more careful study of shell structure and pairing will help resolve the last discrepancy. And we can expect both GCM matrix elements to shrink once the isoscalar pairing amplitude is included as a generator coordinate [73, 74].

#### IV. SUMMARY

We have used covariant multi-reference density functional theory to treat low-lying positive- and negative-parity states in  $^{150}\text{Nd}$  and  $^{150}\text{Sm}$ . The GCM mixes symmetry-projected states with different amounts of quadrupole and octupole deformation. The results indicate that octupole shape correlation have important dynamical effects, including the reduction of quadrupole collectivity in the low-lying states of both nuclei. As for  $0\nu\beta\beta$  decay, static deformation, whether quadrupole or octupole, quenches the nuclear matrix element for that process, but shape fluctuations moderate the effect, so that the inclusion of octupole degrees of freedom ends up reducing the matrix element between the two nuclei considered here by only 7%.

#### Acknowledgements

We are grateful to R. Rodríguez-Guzmán, C. F. Jiao, and L. S. Song for fruitful discussions and to T. R. Rodríguez for providing us the unpublished results of his non-relativistic GCM calculations. Support for this work was provided through the Scientific Discovery through Advanced Computing (SciDAC) program funded by US Department of Energy, Office of Science, Advanced Scientific Computing Research and Nuclear Physics, under Contract No. DE-SC0008641, ER41896, and by the Na-

- [1] J. Argyriades, R. Arnold, C. Augier, J. Baker, A. S. Barabash, A. Basharina-Freshville, M. Bongrand, G. Broudin, V. Brudanin, A. J. Caffrey, E. Chauveau, Z. Daraktchieva, D. Durand, V. Egorov, N. Fatemi-Ghomi, R. Flack, P. Hubert, J. Jerie, S. Jullian, M. Kauer, S. King, A. Klimenko, O. Kochetov, S. I. Kononov, V. Kovalenko, D. Lalanne, T. Lamhamdi, K. Lang, Y. Lemièrre, C. Longuemare, G. Lutter, C. Marquet, J. Martin-Albo, F. Mauger, A. Nachab, I. Nasteva, I. Nemchenok, F. Nova, P. Novella, H. Ohsumi, R. B. Pahlka, F. Perrot, F. Piquemal, J. L. Reyss, J. S. Ricol, R. Saakyan, X. Sarazin, L. Simard, F. Šimkovic, Y. Shitov, A. Smolnikov, S. Snow, S. Söldner-Rembold, I. Štekl, J. Suhonen, C. S. Sutton, G. Szklarz, J. Thomas, V. Timkin, V. Tretyak, V. Umatov, L. Vála, I. Vanyushin, V. Vasiliev, V. Vorobel, and T. Vylov (NEMO Collaboration), *Phys. Rev. C* **80**, 032501 (2009).
- [2] M. Bongrand, *Physics Procedia* **61**, 211 (2015), 13th International Conference on Topics in Astroparticle and Underground Physics, {TAUP} 2013.
- [3] R. F. Casten and N. V. Zamfir, *Phys. Rev. Lett.* **87**, 052503 (2001).
- [4] R. Krücken, B. Albanna, C. Bialik, R. F. Casten, J. R. Cooper, A. Dewald, N. V. Zamfir, C. J. Barton, C. W. Beausang, M. A. Caprio, A. A. Hecht, T. Klug, J. R. Novak, N. Pietralla, and P. von Brentano, *Phys. Rev. Lett.* **88**, 232501 (2002).
- [5] J. Meng, W. Zhang, S. G. Zhou, H. Toki, and L. S. Geng, *Euro. Phys. J. A* **25**, 23 (2005).
- [6] Z. Q. Sheng and J.-Y. Guo, *Mod. Phys. Lett. A* **20**, 2711 (2005).
- [7] T. Nikšić, D. Vretenar, G. A. Lalazissis, and P. Ring, *Phys. Rev. Lett.* **99**, 092502 (2007).
- [8] R. Rodríguez-Guzmán and P. Sarriguren, *Phys. Rev. C* **76**, 064303 (2007).
- [9] T. R. Rodríguez and J. L. Egido, *Phys. Lett. B* **663**, 49 (2008).
- [10] L. M. Robledo, R. R. Rodríguez-Guzmán, and P. Sarriguren, *Phys. Rev. C* **78**, 034314 (2008).
- [11] Z. P. Li, T. Nikšić, D. Vretenar, J. Meng, G. A. Lalazissis, and P. Ring, *Phys. Rev. C* **79**, 054301 (2009).
- [12] W. Urban, R. Lieder, W. Gast, G. Hebbinghaus, A. Krüger-Flecken, K. Blume, and H. Hübner, *Phys. Lett. B* **185**, 331 (1987).
- [13] H. Friedrichs, B. Schlitt, J. Margraf, S. Lindenstruth, C. Wesselborg, R. D. Heil, H. H. Pitz, U. Kneissl, P. von Brentano, R. D. Herzberg, A. Zilges, D. Håger, G. Müller, and M. Schumacher, *Phys. Rev. C* **45**, R892 (1992).
- [14] S. P. Bvumbi, J. F. Sharpey-Schafer, P. M. Jones, S. M. Mullins, B. M. Nyakó, K. Juhász, R. A. Bark, L. Bianco, D. M. Cullen, D. Curien, P. E. Garrett, P. T. Greenlees, J. Hirvonen, U. Jakobsson, J. Kau, F. Komati, R. Julin, S. Juutinen, S. Ketelhut, A. Korichi, E. A. Lawrie, J. J. Lawrie, M. Leino, T. E. Madiba, S. N. T. Majola, P. Maine, A. Minkova, N. J. Ncapayi, P. Nieminen, P. Peura, P. Rahkila, L. L. Riedinger, P. Ruotsalainen, J. Saren, C. Scholey, J. Sorri, S. Stolze, J. Timar, J. Uusitalo, and P. A. Vymers, *Phys. Rev. C* **87**, 044333 (2013).
- [15] W. Nazarewicz and S. L. Tabor, *Phys. Rev. C* **45**, 2226 (1992).
- [16] E. Garrote, J. L. Egido, and L. M. Robledo, *Phys. Rev. Lett.* **80**, 4398 (1998).
- [17] M. Babilon, N. V. Zamfir, D. Kusnezov, E. A. McCutchan, and A. Zilges, *Phys. Rev. C* **72**, 064302 (2005).
- [18] N. Minkov, P. Yotov, S. Drenska, W. Scheid, D. Bonatsos, D. Lenis, and D. Petrellis, *Phys. Rev. C* **73**, 044315 (2006).
- [19] W. Zhang, Z. P. Li, S. Q. Zhang, and J. Meng, *Phys. Rev. C* **81**, 034302 (2010).
- [20] L. M. Robledo and G. F. Bertsch, *Phys. Rev. C* **84**, 054302 (2011).
- [21] R. Rodríguez-Guzmán, L. M. Robledo, and P. Sarriguren, *Phys. Rev. C* **86**, 034336 (2012).
- [22] K. Nomura, D. Vretenar, T. Nikšić, and B.-N. Lu, *Phys. Rev. C* **89**, 024312 (2014).
- [23] K. Nomura, R. Rodríguez-Guzmán, and L. M. Robledo, *Phys. Rev. C* **92**, 014312 (2015).
- [24] P. G. Reinhard, *Rep. Prog. Phys.* **52**, 439 (1989).
- [25] P. Ring, *Prog. Part. Nucl. Phys.* **37**, 193 (1996).
- [26] D. Vretenar, A. Afanasjev, G. Lalazissis, and P. Ring, *Phys. Rep.* **409**, 101 (2005).
- [27] J. Meng, H. Toki, S. Zhou, S. Zhang, W. Long, and L. Geng, *Prog. Part. Nucl. Phys.* **57**, 470 (2006).
- [28] L. S. Geng, J. Meng, and H. Toki, *Chin. Phys. Lett.* **24**, 1865 (2007).
- [29] J.-Y. Guo, P. Jiao, and X.-Z. Fang, *Phys. Rev. C* **82**, 047301 (2010).
- [30] B.-N. Lu, E.-G. Zhao, and S.-G. Zhou, *Phys. Rev. C* **85**, 011301 (2012).
- [31] Z. P. Li, B. Y. Song, J. M. Yao, D. Vretenar, and J. Meng, *Phys. Lett. B* **726**, 866 (2013).
- [32] T. Nikšić, D. Vretenar, and P. Ring, *Phys. Rev. C* **74**, 064309 (2006).
- [33] J. M. Yao, H. Mei, and Z. Li, *Phys. Lett. B* **723**, 459 (2013).
- [34] X. Y. Wu, J. M. Yao, and Z. P. Li, *Phys. Rev. C* **89**, 017304 (2014).
- [35] X. Y. Wu and X. R. Zhou, *Phys. Rev. C* **92**, 054321 (2015).
- [36] J. M. Yao, J. Meng, P. Ring, and D. Vretenar, *Phys. Rev. C* **81**, 044311 (2010).
- [37] J. M. Yao, H. Mei, H. Chen, J. Meng, P. Ring, and D. Vretenar, *Phys. Rev. C* **83**, 014308 (2011).
- [38] J. M. Yao, K. Hagino, Z. P. Li, J. Meng, and P. Ring, *Phys. Rev. C* **89**, 054306 (2014).
- [39] J. M. Yao, E. F. Zhou, and Z. P. Li, *Phys. Rev. C* **92**, 041304 (2015).
- [40] E. F. Zhou, J. M. Yao, Z. P. Li, J. Meng, and P. Ring, *Phys. Lett. B* **753**, 227 (2016).
- [41] J. G. Hirsch, O. Castanos, and P. O. Hess, *Nucl. Phys. A* **582**, 124 (1995).
- [42] K. Chaturvedi, R. Chandra, P. K. Rath, P. K. Raina, and J. G. Hirsch, *Phys. Rev. C* **78**, 054302 (2008).

- [43] D.-L. Fang, A. Faessler, V. Rodin, and F. Šimkovic, *Phys. Rev. C* **82**, 051301 (2010).
- [44] T. R. Rodríguez and G. Martínez-Pinedo, *Phys. Rev. Lett.* **105**, 252503 (2010).
- [45] M. T. Mustonen and J. Engel, *Phys. Rev. C* **87**, 064302 (2013).
- [46] L. S. Song, J. M. Yao, P. Ring, and J. Meng, *Phys. Rev. C* **90**, 054309 (2014).
- [47] J. Terasaki, *Phys. Rev. C* **91**, 034318 (2015).
- [48] J. M. Yao, L. S. Song, K. Hagino, P. Ring, and J. Meng, *Phys. Rev. C* **91**, 024316 (2015).
- [49] B. A. Nikolaus, T. Hoch, and D. G. Madland, *Phys. Rev. C* **46**, 1757 (1992).
- [50] T. Bürvenich, D. G. Madland, J. A. Maruhn, and P.-G. Reinhard, *Phys. Rev. C* **65**, 044308 (2002).
- [51] P. W. Zhao, Z. P. Li, J. M. Yao, and J. Meng, *Phys. Rev. C* **82**, 054319 (2010).
- [52] Y. K. Gambhir, P. Ring, and A. Thimet, *Annals of Physics* **198**, 132 (1990).
- [53] S. J. Krieger, P. Bonche, H. Flocard, P. Quentin, and M. Weiss, *Nucl. Phys. A* **517**, 275 (1990).
- [54] Z. Li, J. Xiang, J. M. Yao, H. Chen, and J. Meng, *Int. J. Mod. Phys. E* **20**, 494 (2011).
- [55] Y. Tian, Z. Ma, and P. Ring, *Phys. Lett. B* **676**, 44 (2009).
- [56] P. Ring and P. Schuck, *The Nuclear Many-Body Problem* (Springer-Verlag, 1980).
- [57] D. L. Hill and J. A. Wheeler, *Phys. Rev.* **89**, 1102 (1953).
- [58] J. J. Griffin and J. A. Wheeler, *Phys. Rev.* **108**, 311 (1957).
- [59] R. Rodríguez-Guzman, J. Egido, and L. Robledo, *Nucl. Phys. A* **709**, 201 (2002).
- [60] D. Lacroix, T. Duguet, and M. Bender, *Phys. Rev. C* **79**, 044318 (2009).
- [61] T. Duguet, M. Bender, K. Bennaceur, D. Lacroix, and T. Lesinski, *Phys. Rev. C* **79**, 044320 (2009).
- [62] V. N. Fomenko, *J. Phys. A: Gen. Phys.* **3**, 8 (1970).
- [63] M. Bender and P.-H. Heenen, *Phys. Rev. C* **78**, 024309 (2008).
- [64] T. R. Rodríguez and J. L. Egido, *Phys. Rev. C* **81**, 064323 (2010).
- [65] F. T. Avignone, S. R. Elliott, and J. Engel, *Rev. Mod. Phys.* **80**, 481 (2008).
- [66] W. C. Haxton and G. J. Stephenson, *Prog. Part. Nucl. Phys.* **12**, 409 (1984).
- [67] F. Šimkovic, G. Pantis, J. D. Vergados, and A. Faessler, *Phys. Rev. C* **60**, 055502 (1999).
- [68] National Nuclear Data Center (NNDC), <http://www.nndc.bnl.gov/>.
- [69] M. Borrajo, T. R. Rodríguez, and J. L. Egido, *Phys. Lett. B* **746**, 341 (2015).
- [70] D.-L. Fang, A. Faessler, and F. Šimkovic, *Phys. Rev. C* **92**, 044301 (2015).
- [71] J. Barea and F. Iachello, *Phys. Rev. C* **79**, 044301 (2009).
- [72] N. L. Vaquero, T. R. Rodríguez, and J. L. Egido, *Phys. Rev. Lett.* **111**, 142501 (2013).
- [73] N. Hinohara and J. Engel, *Phys. Rev. C* **90**, 031301 (2014).
- [74] J. Menéndez, N. Hinohara, J. Engel, G. Martínez-Pinedo, and T. R. Rodríguez, *Phys. Rev. C* **93**, 014305 (2016).